(2) (a) Shea, K. J.; Thompson, F. A.; Pandey, S. D.; Beauchamp, P. S. *J. Am. Chem. Soc.* **1980**, *102*, 3149. (b) Shea, K. J.; Thompson, E. A. *J. Org. Chem.* **1978**, *43*, 4253. (c) Shea, K. J.; Dougherty, T. K., unpublished results.
(3) For general treatments of polymer solvation see: (a) Billmeyer, F. W., Jr. "Textbook of Polymer Science", 2nd ed.; Wiley-Interscience: New York, 1971; p 23. (b) Kwei, T. K. In "Macromolecules: An Introduction to Polymer Science"; Bovey, F. A., Winslow, F. H., Eds.; Academic Press: New York, 1979.
(4) (a) Heitz, W. *Fortschr. Hochpolym.-Forsch.* **1977**, *23*, 1. (b) Funke, W. *Chimica* **1968**, *22*, 111.
(5) (a) Tager, A. A.; Tselepotkina, M. V. *Russ. Chem. Rev. (Engl. Transl.)* **1978**, *47*, 87. (b) Lee, L., Ed. "Characterization of Metal and Polymer Surfaces"; Academic Press: New York, 1977; Vol. I and II.
(6) Turro, N. J. "Modern Molecular Photochemistry"; Benjamin/Cummings: Menlo Park, CA, 1978. (b) Gribault, G., Ed. "Fluorescence: Theory, Instrumentation and Practice"; Marcel Dekker: New York, 1967.
(7) (a) Beavan, S. W.; Hargreaves, J. S.; Phillips, D. *Adv. Photochem.* **1979**, *11*, 207. (b) Chapay, L. L.; DuPre, D. B. *Methods Exp. Phys.* **1980**, *16A*, 404. (c) Edelman, G. M.; McClure, W. O. *Acc. Chem. Res.* **1968**, *1*, 65.
(8) For additional studies of the application of fluorescence spectroscopy to polymer solvation, see: (a) Mikes, F.; Strop, P.; Tuzar, Z.; Labsky, J.; Kalal, J. *Macromolecules* **1981**, *14*, 175. (b) Strop, P.; Mikes, F.; Kalal, J. *J. Phys. Chem.* **1976**, *80*, 694, 702. (c) Chen, H.-L.; Morawetz, H. *Macromolecules* **1982**, *15*, 1445.
(9) Himel, C. M.; Mayer, R. T.; Cook, L. L. *J. Polym. Sci., Part A-1* **1970**, *8*, 2219.
(10) Li, Y.-H.; Chan, L.-M.; Tyer, L.; Moody, R. T.; Himel, C. M.; Hercules, D. M. *J. Am. Chem. Soc.* **1975**, *97*, 3118.
(11) Dimroth, K.; Reichardt, C.; Siepmann, T.; Bohlmann, F. *Justus Liebigs Ann. Chem.* **1963**, *661*, 1.
(12) Hildebrand, J. H.; Scott, R. L. "Regular Solutions"; Prentice-Hall: Englewood Cliffs, NJ, 1962; pp 89-103.
(13) Kosower, E. M. "An Introduction to Physical Organic Chemistry"; Wiley: New York, 1968; p 293.
(14) Kamlet, M. J.; Abboud, J. L. M.; Taft, R. W. *Prog. Phys. Org. Chem.* **1981**, *13*, 485.
(15) (a) Reeves, R. L.; Maggio, M. S.; Costa, L. F. *J. Am. Chem. Soc.* **1974**, *96*, 5917. (b) Coosemans, L.; De Schryver, F. C.; van Dormael, A. *Chem. Phys. Lett., 1979*, *65*, 95.
(16) (a) Kamlet, M. J.; Dickinson, C.; Taft, R. W. *Chem. Phys. Lett.* **1981**, *77*, 69. (b) For a recent comprehensive review of solvent effects, see: Reichardt, C. "Solvent Effects in Organic Chemistry"; Verlag Chemie: New York, 1979.
(17) Lloyd, W. G.; Alfrey, T., Jr. *J. Polym. Sci.* **1962**, *62*, 301.
(18) (a) Millar, J. R.; Smith, D. G.; Kressman, T. R. E. *J. Chem. Soc.* **1965**, 304. (b) Sederel, W. L.; De Jong, G. J. *J. Appl. Polym. Sci.* **1973**, *17*, 2835.
(19) (a) Millar, J. R. *J. Chem. Soc.* **1960**, 1311. (b) Millar, J. R.; Smith, D. G.; Marr, W. E.; Kressman, T. R. E. Ibid. **1963**, *218*, 2779.

Morphology of Random Alternating Block Copolymers of Bisphenol A Polycarbonate and Poly(dimethylsiloxane)

Arthur C. Lind

McDonnell Douglas Research Laboratories, St. Louis, Missouri 63166.
Received April 27, 1983

ABSTRACT: The results of a hydrogen nuclear magnetic resonance study of random alternating block copolymers of bisphenol A polycarbonate (BPAC) and poly(dimethylsiloxane) (DMS) support a proposed domain morphology in which the longest blocks reside at the center and the shortest blocks reside at the surface, with a gradation of block lengths between. The free-induction decay signals from these solid block copolymers contain rapidly decaying Gaussian and slowly decaying Lorentzian components. As the copolymer temperature was increased from 180 to 460 K, the amplitude of the Gaussian component gradually decreased to zero as the BPAC passed through its glass transition. This temperature dependence is attributed to a distribution of BPAC glass transition temperatures caused by a distribution of BPAC block lengths. The data were used to accurately determine the number-average BPAC block lengths and calculate the distributions of BPAC block lengths. The distributions were geometric for copolymers with number-average BPAC block lengths of about 15 but were narrower for copolymers with number-average BPAC block lengths of about 4. The BPAC domain morphology was proposed to explain the ability of BPAC blocks of different lengths to independently undergo motion associated with their individual glass transition temperatures.

Introduction

Block copolymers frequently exhibit phase separation in which blocks of like type associate into domains whose dimensions are on the order of 10 nm. The morphology of monodisperse diblock (AB) and triblock (ABA) copolymers can consist of highly ordered spheres, cylinders, or lamellae, and criteria for phase separation and predictions of domain size and shape have been developed in terms of molecular and thermodynamic variables.[1-5] Random alternating block copolymers (ABAB···ABA) in which both the A and B blocks are polydisperse exhibit a morphology that is generally less ordered, and rigorous calculations for predicting the morphology have not been attempted. Adding to the complexity, the morphology of most block copolymers is strongly dependent upon the solvent from which the sample is cast (i.e., whether the solvent favors A, B, or neither)[6,7] and subsequent heat treatment.[7,8]

When the domain sizes are sufficiently large, their shapes can be easily determined and their sizes can be measured using electron microscopy.[9,10] For smaller sizes, this determination becomes increasingly difficult and other measurement techniques are employed, such as small-angle X-ray scattering,[7,8,10-12] small-angle neutron scattering,[13,14] differential scanning calorimetry (DSC),[15-17] electron paramagnetic resonance,[18] and nuclear magnetic resonance (NMR).[15,19-22] The latter technique was used in this study.

The bisphenol A polycarbonate (BPAC)/poly(dimethylsiloxane) (DMS) block copolymers used in this study are random alternating block copolymers (ABAB··· ABA) having polydisperse blocks.[23] Copolymers having a range of number-average block lengths and compositions were studied. The morphology of these copolymers is thought to vary with composition in the following way. At low BPAC concentrations, the BPAC blocks associate into rigid domains scattered throughout a continuous mobile

0024-9297/84/2217-0300$01.50/0

Table I
Parameters for BPAC/DMS Block Copolymers Determined from Synthesis Conditions

sample[a]	composition[b]	$\overline{x/z} + 2$[c]	$\bar{n}$[d]	$\bar{c}$[e]	$\overline{a/(a-m)}$[f]	$\bar{c}(\overline{a/(a-m)})$[g]	fraction of hydrogen: BPA in DMS blocks	fraction of hydrogen: BPAC blocks	fraction of hydrogen: DMS blocks
35/3.3	35/65	4.7	3.3	20	1.6	32	0.031	0.251	0.718
35/6.5	35/65	7.5	6.5	40	1.2	48	0.007	0.270	0.723
35/15.9	35/65	17.5	15.9	100	1.11	111	0.002	0.268	0.730
50/6.0	50/50	7.0	6.0	20	1.2	24	0.011	0.410	0.579
75/17.7	75/25	18.7	17.7	20	1.06	21	0.002	0.669	0.329

[a] The sample identification scheme is (wt % BPAC)/(BPAC number-average block length, $\bar{n}$). [b] Composition given as (wt % BPAC)/(wt % DMS). The weight of incorporated BPA in the siloxane blocks is included in the weight of the BPAC. [c] Number-average block length of BPAC blocks. [d] Number-average block length of BPAC blocks, counting the BPA incorporated in the siloxane blocks as a BPAC block. [e] Number-average degree of polymerization for DMS. [f] DMS chain extension. [g] Effective block length for DMS.

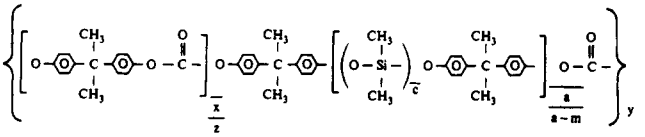

Figure 1. Molecular structure of BPAC/DMS copolymer.

DMS matrix. At large BPAC concentrations, the DMS blocks associate into domains scattered throughout a continuous BPAC matrix.[10,11] The extent to which DMS exists in the BPAC regions, and vice versa, is not clear and was addressed in this study.

The objective of this study was to use hydrogen NMR to characterize the BPAC domains by monitoring the molecular motion associated with their glass transitions. Since the glass transition temperature of a homopolymer is known to be a function of its molecular weight[24] and the glass transition temperature of the BPAC in the subject copolymer, as measured using dynamic mechanical techniques, was found to be a similar function of the BPAC block number-average molecular weight,[7,10] it was anticipated that a distribution of glass transition temperatures, as measured using NMR techniques, could be used to measure the polydispersity of the BPAC block lengths.[25] Also, because the motion associated with the glass transition is cooperative, involving many neighboring molecules, the morphology of the BPAC domains might be revealed from the NMR-measured BPAC block length distributions. Finally, because DSC studies of other copolymers had measured changes in the glass transition temperature that were attributed to the effects of the domain sizes in addition to the effects of the block lengths,[16,26,27] this phenomenon could be examined with NMR for the subject copolymers.

Experimental Procedures

A. Materials and Preparation. The random alternating block copolymers of bisphenol A polycarbonate (BPAC) and poly(dimethysiloxane) (DMS) used in this study were synthesized by H. A. Vaughn[23] and were furnished to us by D. G. LeGrand of the General Electric Research and Development Center. The molecular structure of this block copolymer, following the notation of Niznik and LeGrand,[28] is shown in Figure 1, and the pertinent parameters calculated from the synthesis conditions are listed in Table I. In the first stage of synthesis, m moles of a polydisperse α,ω-dichlorisiloxane oligomer having a number-average degree of polymerization $\bar{c}$ were end capped with a moles of bisphenol A (BPA). During end capping, if a was not much greater than m, BPA was incoporated between siloxane blocks causing chain extension, $\overline{a/(a-m)}$. In the second stage of synthesis, z moles of the end-capped siloxane were reacted with phosgene and x moles of BPA to form polydisperse BPAC blocks in situ. The number-average block length of the BPAC blocks was calculated from overall compositions to be either $\bar{n}$ or $\overline{x/z} + 2$ depending on whether the BPA incorporated in the siloxane blocks was counted as a BPAC block. The weight percent of BPAC in the copolymer includes incorporated BPA. The number-average molecular weight of these copolymers ranged from 28000 to 96000, so that an average chain contained a minimum of three BPAC blocks and two DMS blocks, or a maximum of 41 BPAC blocks and 40 DMS blocks.

Films about 0.005-cm thick were obtained by dissolving the copolymers in $CHCl_3$ and allowing the solvent to evaporate slowly at room temperature in covered petri dishes. These films were heated to 393 K in a vacuum oven for 24 h to remove all solvent and low molecular weight impurities such as cyclic dimethylsilicon tetramer. Samples having a size and shape suitable for NMR measurements were obtained by gently compression molding these films into cylinders 0.32 cm in diameter and 0.6-cm long. The molding was performed in a Pyrex tube to permit visual observation of the sample so that the molding temperatures and pressures did not exceed those necessary to fuse the samples. Molding temperatures were between 430 and 580 K. The molded samples were placed in 5-mm NMR tubes, degassed and annealed for 24 h at 363 K, backfilled with helium at a pressure of 36 kPa, and sealed.

B. Nuclear Magnetic Resonance Measurements. Variable-temperature, pulsed hydrogen NMR measurements were performed on a single-coil spectrometer operating at 100 MHz. An external fluorine lock sample at 94 MHz was used to control the magnet (Varian V-4014) so that small signals could be signal averaged without attendant drift. The 100- and 94-MHz radio-frequency signals were derived from a frequency synthesizer (Hewlett Packard HP5100), and the 8-mT pulsed radio-frequency magnetic field was generated by a programmable digital pulser[29] and a 100-W linear amplifier (Electronic Navagation Industries 3100L). The dead time of the receiver was <6 μs. A transient recorder (Biomation 826) in conjunction with a signal averager (Nicolet 1070) was used to acquire and store the signals, and a computer (Digital Equipment PDP-8) was used to analyze the signals.

The free-induction NMR signal following a single 90° pulse was decomposed into a Gaussian signal and a Lorentzian signal, viz.

$$S(t) = A_G \exp(-t/T_{2G})^2 + A_L \exp(-t/T_{2L}) \quad (1)$$

Generally, the Gaussian signal amplitude A_G is proportional to the number of hydrogens in rigid molecules (below the glass transition temperature), and the Lorentzian signal amplitude A_L is proportional to the number of hydrogens in mobile molecules undergoing liquid-like motion (above the glass transition temperature). It was anticipated that the fraction of rigid hydrogens, $F = A_G/(A_G + A_L)$, would be a measure of the number of BPAC blocks below their glass transition temperature.

Experimental Results

The free-induction decay signals of the BPAC/DMS block copolymers were obtained as a function of temperature from 180 to 460 K. Between these temperature limits, the signals contained two components, a Gaussian having T_{2G} between 20 and 30 μs and a Lorentzian having

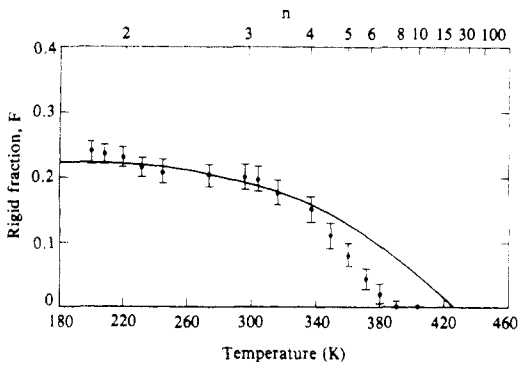

Figure 2. Temperature dependence of the rigid fraction for the 35/3.3 sample. The solid line is calculated assuming a binomial distribution.

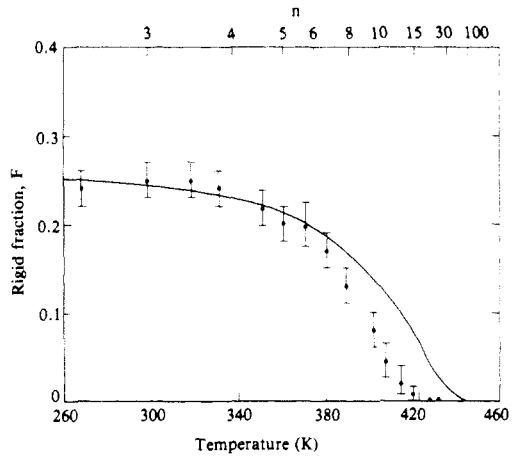

Figure 3. Temperature dependence of the rigid fraction for the 35/6.5 sample. The solid line is calculated assuming a binomial distribution.

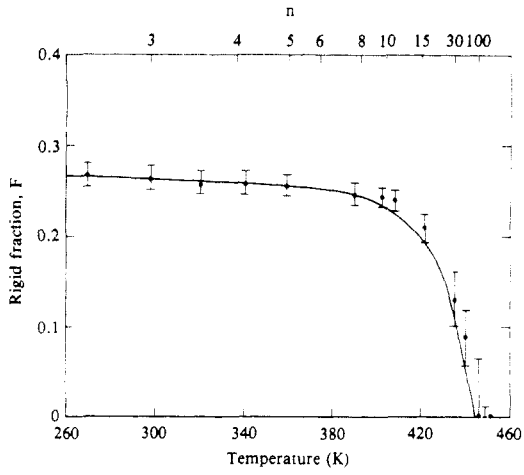

Figure 4. Temperature dependence of the rigid fraction for the 35/15.9 sample. The solid line is calculated assuming a binomial distribution.

T_{2L} between 600 and 2500 μs. These large differences in relaxation times of the two components facilitated a unique decomposition of the free-induction decay signals.[22]

The rigid (Gaussian) fraction, $F = A_G/(A_G + A_L)$, is plotted in Figures 2–6 as a function of temperature for the five block copolymers studied. Because thermal history might affect the domain structure of these block copolymers, it is important to note that the temperature measurements were not necessarily taken in any particular order, and the samples were always returned to room temperature after each temperature measurement. The measurements were repeated on different days, and the

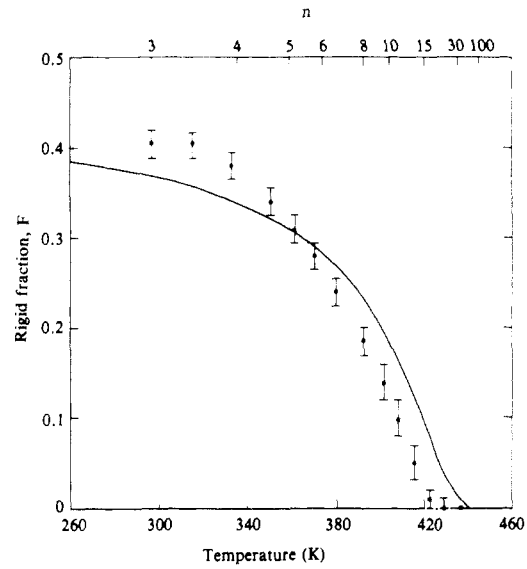

Figure 5. Temperature dependence of the rigid fraction for the 50/6.0 sample. The solid line is calculated assuming a binomial distribution.

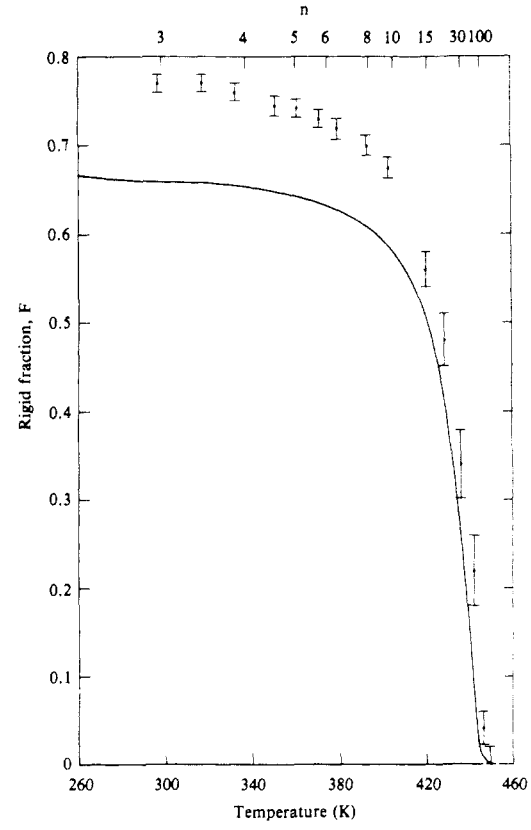

Figure 6. Temperature dependence of the rigid fraction for the 75/17.7 sample. The solid line is calculated assuming a binomial distribution.

error bars represent the root mean square deviation of the results. Within experimental error, no thermal history effects were observed.

Analyses of Experimental Results

A. Overview. Figures 2–6 show that the rigid fraction decreases with an increase in temperature. This decrease was interpreted as the result of the onset of extensive molecular motion of the BPAC as it passed through its glass transition temperature. At low temperatures, the measured rigid fraction is within 0.02 of the calculated fraction of hydrogens in the BPAC blocks, as presented in Table I, except for the 75/17.7 sample. This implies

that within experimental error, at moderately low temperatures, all BPAC blocks in these samples (except 75/17.7) are associated in rigid domains, and few if any BPAC blocks are located in the mobile DMS matrix. The measured rigid fraction for the 75/17.7 sample is 0.77, while the calculated fraction of hydrogens in BPAC is only 0.669. Evidently the domain structure of this BPAC-rich copolymer is such that the BPAC matrix immobilizes some of the DMS, thereby increasing the measured rigid fraction.

Figures 2–6 also show that the glass transition temperature of the BPAC increases with an increase in the BPAC block length. A similar result was obtained by Kambour,[7,10] who performed 1-Hz dynamic mechanical measurements on BPAC/DMS block copolymers that showed the presence of two loss peaks, one corresponding to the glass transition of the DMS blocks at 163 K and the other corresponding to the glass transition of the BPAC blocks. The measured glass transition temperature T_g of the BPAC blocks was related to the number-average length of the BPAC blocks $\bar{n}$ in the following way:[7,10]

$$T_g(\bar{n}) = 421 - 457/\bar{n} \tag{2}$$

This relation is similar to the Flory–Fox[24] relation for homopolymers, which is based on the concept of free volume provided by the chain ends and suggested to Kambour[7,10] that the BPAC blocks acted as though they were free ended because of the large mobility of the attached DMS blocks.

Niznik and LeGrand[28] pursued this idea and hypothesized that because the BPAC block lengths were polydisperse, each individual BPAC block would exhibit a glass transition temperature governed by its length. The wide temperature range over which the rigid fraction decreases to zero, as shown in Figures 2–6, supports this hypothesis. The first analysis presented below is based on this hypothesis. However, because the molecular motion associated with the glass transition is a cooperative motion involving many neighboring molecules, it is reasonable to assume that the glass transition temperature of a particular BPAC block should be a function of its block length appropriately averaged with the block lengths of its many neighbors. The second analysis presented below takes this averaging into consideration.

The first analysis attempts to fit the experimental data with results of a model calculation. The model assumes that the BPAC block lengths are binomially distributed and the glass transition temperature of any BPAC block is a function of its length alone, and not a function of the lengths of its neighbors. An equivalent assumption for this analysis is that the glass transition temperature of any BPAC block is a function of its length and the lengths of its neighbors which all happen to have the same length (segregation of like lengths). This first analysis allows a direct comparison of experimental data with results of a model calculation based on Niznik and LeGrand's[28] original hypothesis.

The second analysis calculates "average" block length distributions from the experimental data. The term "average" acknowledges the fact that the experimental data are a function of an appropriate average of many neighboring blocks participating in the cooperative molecular motion associated with the glass transition. An estimate of the number of blocks participating in the cooperative motion is achieved by comparing the experimentally determined block length distributions with averages of one or more binomial distributions.

B. Comparison of Experimental Results with Model Calculation. This analysis attempts to fit the experimental data with results of a model that assumes that the BPAC blocks are binomially distributed and the glass transition temperatures of the individual BPAC blocks are given by a relation like that of eq 2. However, because Kambour's mechanical measurements are sensitive to molecular motions occurring near 1 Hz, whereas the hydrogen NMR measurements are sensitive to molecular motions occurring near 10 kHz, the intercept temperature (421 K) in eq 2 was expected to be different for the NMR measurements. The appropriate temperature was determined from the temperature dependence of the spin–spin relaxation time T_{2G} for a high molecular weight (≈40 000) polycarbonate homopolymer. For this homopolymer, T_{2G} increased abruptly at 450 K (from <45 μs at 444 K to >140 μs at 456 K), so the appropriate NMR glass transition temperature relation was taken to be

$$T_g(n) = 450 - 457/n \tag{3}$$

where $T_g(n)$ is the glass transition temperature of a BPAC block containing n monomers. There are two differences between eq 2 and 3. The first difference is the intercept temperature. The second is that eq 2 assumes that all the BPAC domains have the same glass transition temperature governed by the number-average BPAC block length in the bulk sample, whereas eq 3 assumes that each BPAC block in the sample has a glass transition temperature governed by its block length. Equation 3 was used to construct the scale at the top of Figures 2–6 which indicates the length n of the BPAC block whose glass transition temperature is equal to the temperature appearing directly below on the temperature scale.

A binomial distribution of BPAC block lengths is assumed because under ideal polymerization conditions it is expected.[30,31] If the distribution of BPAC block lengths is given by the binomial distribution

$$N(n) = \frac{1}{\bar{n}}\left(1 - \frac{1}{\bar{n}}\right)^{n-1} \tag{4}$$

then the fraction $F(T)$ of hydrogens contained in the rigid BPAC blocks at any temperature can be obtained from

$$F(T) = \frac{f}{\bar{n}} \sum_{n=457/(450-T)}^{\infty} nN(n) \tag{5}$$

where f is the fraction of all copolymer hydrogens that are contained in the BPAC and BPA as given in Table I (assuming BPA can associate with BPAC in domains). The result of the summation is

$$F(T) = f\left(1 + \frac{1}{\bar{n}}\frac{457}{450 - T}\right)\left(1 - \frac{1}{\bar{n}}\right)^{457/(450-T)} \tag{6}$$

Curves derived from this equation, using values of f and $\bar{n}$ given in Table I, are plotted in Figures 2–6, where comparisons with the experimental data can be made. While there is general agreement, the differences are significantly greater than the experimental errors. In general, the experimentally determined rigid fractions $F(T)$ decrease more rapidly with temperature than do the results of the model calculations. This result implies that the actual block length distribution is narrower than a binomial distribution or the cooperative motion of neighboring BPAC blocks causes averaging which narrows the effective distribution. The extent of this averaging is examined more quantitatively in the second analysis which follows.

C. Experimentally Determined Distribution of Block Lengths. As an alternative to the preceding analysis, which involved calculating the temperature dependence of the rigid fraction from an assumed BPAC

Table II
Comparison of Number-Average BPAC Block Lengths

sample	composition[a]	$\bar{n}$ from synthesis conditions	$\bar{n}_e$ from analysis of NMR data
35/3.3	35/65	3.3	3.1
35/6.5	35/65	6.5	6.2
35/15.9	35/65	15.9	17.4
50/6.0	50/50	6.0	6.3
75/17.7	75/25	17.7	19.2

[a] Given as (wt % BPAC)/(wt % DMS).

block length distribution and eq 3, the block length distribution is calculated from the experimentally measured temperature dependence of the rigid fraction and eq 3. If $N_e(n)$ is the experimentally determined distribution of BPAC block lengths, then, as in eq 5, the rigid fraction is proportional to the fraction of hydrogens contained in those BPAC blocks having a glass transition temperature greater than the measurement temperature, viz.

$$F(T) = \frac{f}{\bar{n}_e} \sum_{n=457/(450-T)}^{\infty} nN_e(n) \tag{7}$$

where $\bar{n}_e$ is the number-average block length of the $N_e(n)$ distribution function. $N_e(n)$ and $\bar{n}_e$ are determined from the experimentally measured $F(T)$ by calculating the contribution each term in eq 7 makes to $F(T)$, viz.

$$\frac{nN_e(n)}{\bar{n}_e} = \frac{1}{f}\left[F\left(450 - \frac{457}{n}\right) - F\left(450 - \frac{457}{n+1}\right)\right] \tag{8a}$$

for $n = 2, 3, 4 \ldots$, and

$$\frac{nN_e(n)}{\bar{n}_e} = \frac{1}{f}\left[f - F\left(450 - \frac{457}{n+1}\right)\right] \tag{8b}$$

for $n = 1$. These equations yield the ratios $nN_e(n)/\bar{n}_e$; $\bar{n}_e$ is obtained by using the normalization relation

$$\sum_{n=1}^{\infty} N_e(n) = 1 \tag{9}$$

When eq 8 and 9 are used to calculate $N_e(n)$ and $\bar{n}_e$, the quantity f can be determined from the known copolymer composition as given in Table I or it can be determined from the low-temperature limit of $F(T)$. In the results that follow, f was determined from the copolymer composition, except for the 75/17.7 sample where f was determined from the low-temperature limit of $F(T)$.

To facilitate the use of eq 8, the experimental data had to be interpolated by drawing smooth curves through the error bars, this procedure was repeated several times to obtain estimates of the uncertainty in the calculated values of $nN_e(n)$. For some samples, experimental data were not obtained at a sufficiently low temperature to calculate $N_e(1)$ from eq 8b; in these cases a reasonable estimate was obtained by using the data at the lowest measurement temperature.

The experimentally determined number-average BPAC block lengths $\bar{n}_e$ are presented in Table II where they are compared with those predicted from the copolymer synthesis conditions. The results in Table II are in good agreement, which demonstrates that, like the dynamic mechanical measurements,[7,10] the NMR measurements are capable of determining the number-average BPAC block lengths when analyzed with a Flory–Fox[24] relation (eq 3).

The experimentally determined BPAC block length distributions $nN_e(n)$ are presented in Figures 7–11, where they are compared with averages of one or more binomial distributions. Experimental points were determined for

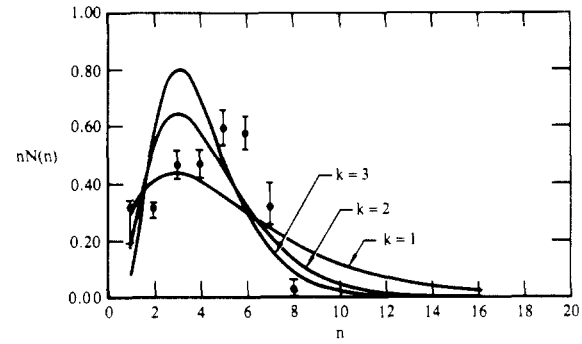

Figure 7. BPAC block length distribution calculated from NMR data for the 35/3.3 sample. The solid lines are averages of k binomial distributions.

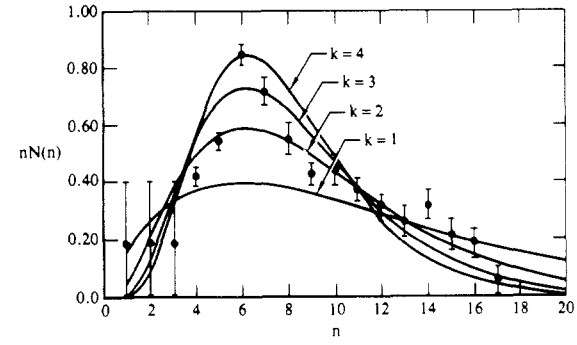

Figure 8. BPAC block length distribution calculated from NMR data for the 35/6.5 sample. The solid lines are averages of k binomial distributions.

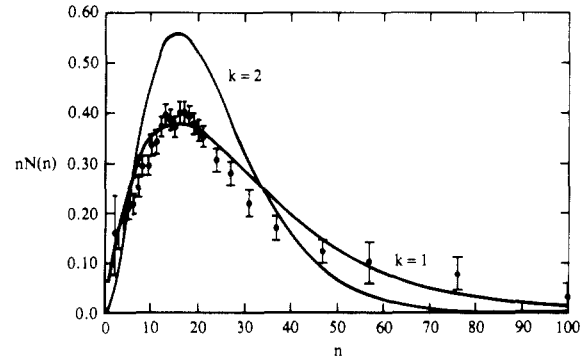

Figure 9. BPAC block length distribution calculated from NMR data for the 35/15.9 sample. The solid lines are averages of k binomial distributions.

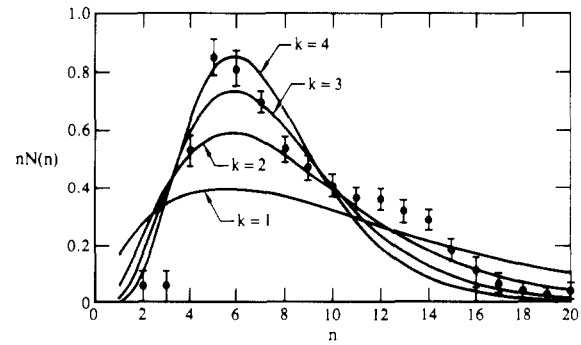

Figure 10. BPAC block length distribution calculated from NMR data for the 50/6.0 sample. The solid lines are averages of k binomial distributions.

all values of n, but for clarity only selected points are shown. Because the molecular motion associated with the glass transition is a cooperative motion involving many neighboring blocks, it is reasonable to assume that each

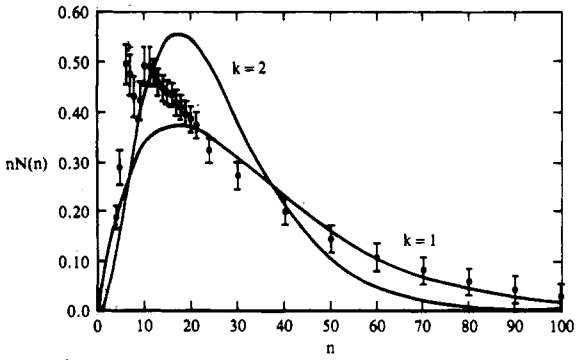

Figure 11. BPAC block length distribution calculated from NMR data for the 75/17.7 sample. The solid lines are averages of k binomial distributions.

BPAC domain has a glass transition temperature that is governed by the number-average block length of the BPAC blocks contained in it. Therefore, the distribution of the number-average block lengths in the domains is calculated for comparison with the experimentally determined distribution. If each of the BPAC domains in a BPAC/DMS block copolymer is composed of k BPAC blocks and the lengths of the BPAC blocks are described by a binomial distribution having a number average of $\bar{n}$, then the resulting distribution of the total number of segment lengths n in a domain is

$$N(n,\bar{n},k) = \frac{(n-1)!}{(k-1)!\,(n-k)!}\,\frac{1}{\bar{n}^k}\left(1-\frac{1}{\bar{n}}\right)^{n-k} \qquad (10)$$

Since n is the total segment length in a domain, the number-average length of a block in a domain containing k blocks is n/k; this scale factor was applied to eq 10 to generate the curves plotted in Figures 7–11 for comparison with the experimentally determined BPAC block length distributions (for clarity, continuous curves are drawn rather than discrete points). As k increases, more averaging takes place within the domains causing them to become more alike, and the distribution function narrows.

In some cases the experimental distributions and the average of binomial distributions agree when $k = 1$, e.g., samples 3.5/15.9 (Figure 9) and 75/17.7 (Figure 11). The excessive number of short BPAC blocks experimentally determined for the BPAC-rich sample 75/17.7 was undoubtedly caused by BPAC blocks which surrounded and immobilized some DMS blocks, causing them to be erroneously counted as rigid BPAC blocks. In other cases, agreement was obtained when $k = 3$ or 4, e.g., sample 50/6 (Figure 10). Reasonable agreement occurs in all five samples when $k \leq 4$.

Four is an unusually small number of blocks per domain when compared with estimates obtained from other experimental studies. Transmission electron microscopy[7] of block copolymers similar to samples 35/6.5 and 35/15.9 have produced micrographs showing irregularly shaped BPAC domains having sizes of 7.3 and 18.4 nm, respectively. By approximating the irregular shapes as spheres composed of BPAC having a density of 1.2 g/cm^3 and a monomeric weight of 254 g/mol, calculations show that these domains contain 89 and 580 BPAC blocks, respectively. Small-angle neutron scattering studies[32] of the 50/6 sample yielded a domain size of about 9.6 nm from which one calculates 220 BPAC blocks in each domain. The agreement between the transmission electron microscopy and small-angle neutron scattering data provides conclusive evidence that these BPAC domains contain more than 50 blocks. When $k \geq 50$, the distribution function (eq 10) is very narrow, and a very narrow distribution in glass transition temperatures is expected. However, broad distributions of glass transition temperatures (block lengths) were measured with NMR, and this discrepancy requires explanation. In the following section explanations based on the BPAC domain morphology are examined.

While the following section concerns domain morphology effects, which are important to interpretation of these NMR results, the actual BPAC block length distribution functions for these copolymers are not known. Pebbles[30] has shown that under ideal conditions, a single-stage polymerization produces a binomial distribution, and under certain conditions a two-stage polymerization produces a narrower distribution than the binomial distribution. Since a two-stage polymerization was used to synthesize these copolymers, it is possible that the narrow distributions calculated from the NMR data for some of these copolymers are to be expected.

Discussion of Results in Terms of Domain Morphology

A. Domains Containing Blocks of Like Length. One possible explanation for the observed lack of significant averaging (narrowing of the distribution) is that when the BPAC domains were being formed during solvent evaporation, the BPAC blocks selectively entered domains that contained blocks of like length. Thus, each domain would contain blocks having only one length, causing the domains to have a wide distribution of glass transition temperatures consistent with the observed NMR results. However, this explanation is rejected because the constraints placed upon the BPAC blocks by the attached DMS blocks make this high degree of ordering of BPAC blocks improbable.

B. Domain Size Effects. Another explanation concerns the influence that domain size may have on the glass transition because of the effects of surface energy and the mixing of domain and matrix material in the interface.[16,26,27] Thus, in addition to the reduction in glass transition temperature caused by BPAC block length, n, effects, an additional reduction might be caused by surface effects, viz.

$$T_g(\bar{n}, s) = T_{g_\infty} - \frac{K_n}{\bar{n}} - K_s\frac{s}{v} \qquad (11)$$

where s/v is the surface to volume ratio of the domains and K_n and K_s are constants. Equation 11 has been used successfully to explain data for styrene/butadiene/styrene triblock copolymers.[26] The best fit to published data relating molecular weight and glass transition temperature for the polycarbonate homopolymer, where $K_s \equiv 0$, yields $T_{g_\infty} = 429$ K and $K_n = 400$ K,[33,34] while Kambour's data for the copolymer, if K_s is assumed to be zero, yields $T_{g_\infty} = 421$ K and $K_n = 457$ K, as in eq 3. The slightly larger value of K_n for the copolymer indicates that the glass transition temperature of the copolymer is reduced slightly more than that of the homopolymer for the same reduction in BPAC block length. Kambour[7] claims that this difference can be explained in a number of ways: e.g., (1) the difference in techniques for measuring the glass transition temperatures (stress relaxation,[33] differential thermal analysis,[34] and mechanical relaxation[7]), (2) hydroxyl end groups on the homopolymer that could associate through hydrogen bonding and increase the effective chain length, whereas such associations could not occur in the copolymer, and (3) the presence of a small quantity of DMS in the BPAC domains acting as plasticizers to lower the T_g of the domains.

If the difference is attributed to a surface-to-volume ratio effect, the magnitude of the effect can be assessed by

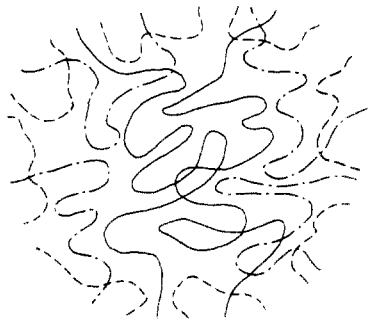

Figure 12. Proposed BPAC domain morphology in which the longest blocks (solid lines) reside in the center and the shortest blocks (dashed lines) reside at the surface, with a gradation of block lengths (dot–dashed lines) between. The attached DMS blocks outside of the domain are not shown.

letting K_n for the copolymer be equal to K_n for the homopolymer, and calculating K_s from data for one of the copolymers whose surface-to-volume ratio is known from transmission electron microscopy. By use of the 35/6.5 sample with its known 7.3-nm domain size,[7] s/v is 0.82 nm^{-1}, and K_s is calculated to be 10.7 K nm, if T_{g_∞} is kept at 421 K as in eq 2. To test the validity of these constants, the T_g for sample 35/15.9 is calculated. For this sample the domain size is 18.4 nm and the glass transition temperature is calculated to be 392 K, which is exactly the same temperature calculated using eq 2 with no surface term. This agreement is somewhat accidental inasmuch as the increase in block length was accompanied by similar increase in domain volume to surface ratio.

While these results do not resolve whether surface-to-volume effects should be included in the expression for calculating the glass transition temperature, they do provide sufficient information for calculating whether the distribution in NMR-measured glass transition temperatures could be caused by a distribution in domain sizes. Because the transmission electron micrographs of these samples showed that within any one sample, the diameters of the irregularly shaped domains were of uniform size (≥3 nm), varying at most by a factor of 2 or 3, the surface-to-volume ratio term $K_s(s/v)$ could contribute at most a 21.4 K distribution in the measured glass transition temperature. The distributions in T_g actually measured with NMR were more than 120 K, e.g., see Figures 2–6. As a result, we conclude that the measured distributions in T_g cannot be explained by domain size effects alone.

C. Graded Domain Morphology. The most plausible explanation is that as the solvent evaporates, the long BPAC blocks precipitate first, followed by the shorter blocks. This process would produce domains in which the longest blocks are at the center and the shortest blocks are at the surface, with a gradation of block lengths between, as shown in Figure 12. This domain morphology is consistent with the NMR results because as the temperature is increased to the glass transition temperature of the shortest BPAC blocks, they are at the surface and are free to move without the immobilizing restrictions of the longer BPAC blocks. As the temperature is increased further, each new layer of longer BPAC blocks is free to undergo the motion associated with its glass transition. This morphology results in a range of glass transition temperatures for each domain rather than a single glass transition temperature for each domain governed by the average BPAC block length in the domain.

Another argument, supporting the graded domain morphology shown in Figure 12 can be made. The moderately low-temperature (~200 K) NMR measurements of all of the samples (except sample 75/17.7, as previously explained) are consistent with the view that, within experimental error, all BPAC is in rigid domains and all DMS is in the mobile matrix. The transmission electron microscopy[7] and neutron scattering[32] measurements show that the rigid domain sizes are relatively large. As a typical example, using transmission electron microscopy, the measured size of the domain in the 35/6.5 sample is 7.3 nm, while the stretched-out (not random walk) end-to-end distance of a BPAC block having a degree of polymerization of 6.5 is 6.5 times the 1.16-nm length of a single monomer unit,[35] or 7.5 nm. Thus, while an average BPAC block could extend from the surface of the domain, through the center, and back to the surface, the shorter blocks could not exist at the center of the domain without pulling some of the attached DMS into the rigid domain. Because the NMR results strongly suggest that the DMS is completely mobile, we conclude that the short BPAC blocks cannot be at the center of the domains and that the morphology of the domains must be similar to that shown in Figure 12.

Conclusions

The NMR results for copolymers containing ≤50 wt % BPAC showed that at moderately low temperatures (~200 K) the fraction of hydrogens contained in rigid molecules is equal to the fraction of hydrogens contained in the BPAC, suggesting that virtually all BPAC is in rigid domains and virtually all DMS is in the mobile matrix. The rigid fraction in a copolymer containing 75 wt % BPAC is greater than the fraction of hydrogens in the BPAC, indicating that some of the DMS is immobilized by the BPAC. The temperature dependence of the rigid fraction was interpreted in terms of a distribution in glass transition temperatures resulting from a distribution in BPAC block lengths and the surface-to-volume ratios of the BPAC domains. It was not possible to determine if the surface-to-volume ratio of a domain affects the glass transition temperature because experimental data were not available in which the block lengths and surface-to-volume ratios varied independently. However, an upper limit was set on the surface-to-volume effect, and it was small compared with the block length effect for the copolymers studied. Therefore, the data were interpreted in terms of block length effects. The data were used to accurately calculate the number-average BPAC block lengths of the samples and determine the distributions of BPAC block lengths. These distributions were either binomial or slightly narrower than binomial, which would be expected for the two-stage polymerization procedure used to synthesize these copolymers. To explain the ability of the BPAC blocks of different lengths to independently undergo motion associated with their individual glass transition temperatures, a BPAC domain morphology was proposed in which the longest blocks reside at the center and the shortest blocks reside at the surface, with a gradation of block lengths between.

Acknowledgment. This research was conducted in part under Naval Air Systems Command Contract N00019-76-C-0565 and in part under the McDonnell Douglas Independent Research and Development Program. I gratefully acknowledge helpful discussions with D. P. Ames, I. M. Brown, R. L. Levy, M. H. Litt, and T. C. Sandreczki.

References and Notes

(1) Helfand, E.; Wasserman, Z. R. *Macromolecules* **1978**, *11*, 960 and prior work cited therein.
(2) Krause, S. *J. Polym. Sci., Polym. Phys. Ed.* **1975**, *13*, 1975 and prior work cited therein.

(3) Leary, D. F.; Williams, M. C. *J. Polym. Sci., Part B* **1970**, *B8*, 335.
(4) LeGrand, D. G. *Polym. Prepr., Am. Chem. Soc., Div. Polym. Chem.* **1970**, *11*, 434.
(5) Meier, D. J. *Appl. Polym. Symp.* **1974**, 24, 67 and prior work cited therein.
(6) Bajaj, P.; Varshney, S. K. *Polymer* **1980**, *21*, 201.
(7) Kambour, R. P. "Block Copolymers"; Aggarwal, S. L., Ed.; Plenum Press: New York-London, 1970; p 263.
(8) Wilkes, G. L.; Emerson, J. A. *J. Appl. Phys.* **1976**, *47*, 4261.
(9) Aggarwal, S. L. *Polymer* **1976**, *17*, 938.
(10) Kambour, R. P. *J. Polym. Sci., Part B* **1969**, *B7*, 573.
(11) LeGrand, D. G. *J. Polym. Sci., Part B* **1969**, *B7*, 579.
(12) Hashimoto, T.; Fujimura, M.; Kawai, H. *Macromolecules* **1980**, *13*, 1660.
(13) Richards, R. W.; Thomason, J. L. *Polymer* **1981**, *22*, 581.
(14) Russell, T. P.; Stein, R. S. *J. Polym. Sci.* **1982**, *20*, 1593.
(15) Morêse-Séguéla, B.; St.-Jacques, M.; Renard, J. M.; Prud'homme, J. *Macromolecules* **1980**, *13*, 100.
(16) Gaur, U.; Wunderlich, B. *Macromolecules* **1980**, *13*, 1618.
(17) Krause, S.; Iskandar, M. *Adv. Chem. Ser.* **1979**, *No 176*, 205.
(18) Brown, I. M. *Macromolecules* **1981**, *14*, 801.
(19) LeGrand, D. G. *J. Rheol. (N. Y.)* **1971**, *15*, 541.
(20) Assink, R. A. *Macromolecules* **1978**, *11*, 1233.
(21) Lind, A. C. *J. Chem. Phys.* **1977**, *66*, 3482.
(22) Wardell, G. E.; McBrierty, V. J.; Douglass, D. C. *J. Appl. Phys.* **1974**, *45*, 3441.
(23) Vaughn, H. A., Jr. *J. Polym. Sci., Part B* **1969**, *B7*, 569.
(24) Fox, T. G.; Flory, P. J. *J. Appl. Phys.* **1950**, *21*, 581.
(25) Lind, A. C. *Bull. Am. Phys. Soc.* **1980**, *25*, 315.
(26) Bares, J. *Macromolecules* **1975**, *8*, 244.
(27) Couchman, P. R.; Karasz, F. E. *J. Polym. Sci., Polym. Symp. Ed.* **1978**, *63*, 271.
(28) Niznik, G. E.; LeGrand, D. G. *J. Polym. Sci., Polym. Symp. Ed.* **1977**, *60*, 97.
(29) Lind, A. C. *Rev. Sci. Instrum.* **1972**, *43*, 1800.
(30) Pebbles, L. H., Jr. *Macromolecules* **1976**, *9*, 58.
(31) For the BPAC/DMS synthesis conditions employed here, the $n = 1$ BPA blocks were formed during end capping, while the $n \geq 2$ BPAC blocks were independently formed during the second stage of polymerization. A modified binomial distribution function incorporating these features was employed, but the errors in the NMR data did not justify its use.
(32) Desa, J. A. E.; Brown, I. M.; Lind, A. C.; Sandreczki, T. C. *Am. Crystallogr. Assoc., Ser. 2* **1983**, *11*, 36.
(33) Mercier, J. P.; Aklonis, J. J.; Litt, M.; Tobolsky, A. V. *J. Appl. Polym. Sci.*, **1965**, *9*, 447.
(34) Merrill, S. H.; Petrie, S. E. *J. Polym. Sci., Part A* **1965**, *3*, 2189.
(35) Williams, A. D.; Flory, P. J. *J. Polym. Sci., Part A-2* **1968**, *6*, 1945.

Phase Diagrams and Morphology of a Urethane Model Hard Segment and Polyether Macroglycols

Kirk K. S. Hwang,† David J. Hemker, and Stuart L. Cooper*

Department of Chemical Engineering, University of Wisconsin, Madison, Wisconsin 53706.
Received May 19, 1983

ABSTRACT: Binary mixtures of a urethane hard-segment model compound, diethyl 4,4′-methylenebis(*N*-phenylcarbamate) (H_1), and various polyether macroglycols have been investigated by means of differential scanning calorimetry, wide-angle X-ray diffractometry, and optical microscopy. Both poly(ethylene oxide) (1500 MW) and poly(tetramethylene oxide) (1000 MW) form a eutectic with H_1 in weight ratios of H_1/PEO (40/60) and H_1/PTMO (20/80). Poly(propylene oxide) and H_1 mix to form a crystalline–amorphous blend. X-ray diffraction patterns showed that the presence of polyether macroglycols caused no change in the crystal structure of H_1 crystals in the blends. This suggests that the melting point depression observed is explicable in terms of H_1–polyol thermodynamic mixing. On the basis of Scott's equation, the interaction parameter densities of H_1/PEO, H_1/PTMO, and H_1/PPO were determined to be −4.63 cal/cm^3, −3.42 cal/cm^3, and −1.21 cal/cm^3, respectively, at the H_1 melting point. Optical microscopy revealed that H_1 spherulites were larger in size and more perfect in texture in the blends of H_1 and polyols than in pure H_1.

Introduction

The morphology and physical properties of diphenylmethane diisocyanate (MDI) based segmented polyurethanes have been studied extensively[1-4] and have been found to depend on several factors such as the composition ratio of urethane and polyether segments, the molecular weight of the individual segments, and segmental compatibility.

In this study, the segmental compatibility of urethane hard segments and polyether soft segments was investigated by determining the phase diagrams of physical mixtures of a model hard segment with various macroglycols. Diethyl 4,4′-methylenebis(*N*-phenylcarbamate) (designated as H_1), which is the repeating unit of the MDI–butanediol (BD) hard segment, served as the hard-segment model compound. Poly(ethylene oxide) (PEO), poly(propylene oxide) (PPO), and poly(tetramethylene oxide) (PTMO) macroglycols were used to model the soft segment.

A recent study by Camberlin[5] showed that the hard-segment model compound diethyl 4,4′-methylenebis(*N*-phenylcarbamate) displays a melting point of 125 °C in its initial stable form and 99.7 °C in its metastable form. Blackwell[6] studied a similar model compound of the urethane hard segment, dimethyl 4,4′-methylenebis(*N*-phenylcarbamate), using X-ray diffraction. This model compound was found to possess a monoclinic structure with four molecules in each unit cell. However, he also reported an oriented MDI/BD hard segment in a triclinic structure.[7,8]

The crystalline structures of poly(ethylene oxide) (PEO) and poly(tetramethylene oxide) (PTMO) have been studied extensively by a number of authors using X-ray scattering and IR spectroscopy.[9-12] PEO was found to possess a monoclinic helical structure with four repeating units in each unit cell, and PTMO was found to possess a planar zigzag monoclinic structure with two repeating units in each unit cell. Atactic poly(propylene oxide) is an amorphous material.

When two crystalline polymers or one crystalline and one amorphous polymer are mixed together, the miscibility of the two components with respect to composition and

† Present address: Life Sciences Sector Lab, 3M Co., St. Paul, MN 55144.

0024-9297/84/2217-0307$01.50/0